**Article ID:** 1000-324X(2023)06-0693-08 **DOI:** 10.15541/jim20220551

# Enhanced Compatibility and Activity of High-entropy Double Perovskite Cathode Material for IT-SOFC

GUO Tianmin[1], DONG Jiangbo[2], CHEN Zhengpeng[2], RAO Mumin[2], LI Mingfei[2], LI Tian[1], LING Yihan[1]

(1. School of Materials Science and Physics, China University of Mining and Technology, Xuzhou 221116, China; 2. Guangdong Energy Group Science and Technology Research Institute Co., Ltd., Guangzhou 510000, China)

**Abstract:** Intermediate-temperature solid oxide fuel cell (IT-SOFC) is promising for carbon neutrality, but its cathode is limited by the contradiction between thermal compatibility and catalytic activity. Herein, we propose a high-entropy double perovskite cathode material, $GdBa(Fe_{0.2}Mn_{0.2}Co_{0.2}Ni_{0.2}Cu_{0.2})_2O_{5+\delta}$ (HE-GBO) with improved compatibility and activity, in view of the high-entropy strategy by multi-elemental coupling, which possesses double perovskite structure and excellent chemical compatibility with state-of-the-art $Gd_{0.1}Ce_{0.9}O_{2-\delta}$ (GDC). The polarization resistance ($R_p$) of the symmetrical cells with HE-GBO cathode is 1.68 $\Omega\cdot cm^2$ at 800 ℃, and the corresponding $R_p$ of HE-GBO-GDC (mass ratio 7:3) composite cathode can be greatly reduced (0.23 $\Omega\cdot cm^2$ at 800 ℃) by introducing GDC. Dendritic microchannels anode-supported single cells with HE-GBO and HE-GBO-GDC cathodes realize maximum power densities of 972.12 and 1057.06 mW/cm$^2$ at 800 ℃, respectively, indicating that cell performance can be enhanced by high-entropy cathodes. The results demonstrate that high-entropy double perovskite cathode material HE-GBO has a high potantial to solve the conflict problem of thermal compatibility and catalytic activity in IT-SOFCs.

**Key words:** high-entropy cathode; solid oxide fuel cells; thermal compatibility; dendritic microchannels

The transformation of chemical energy to electrical energy can be realized through solid oxide fuel cells (SOFCs) with the advantages of high conversion efficiencies, extensive fuel sources, and low emission, as compared with other energy technologies[1-2]. Over the last few decades, the common operating condition of SOFCs is 800–1000 ℃. High operating temperature of SOFCs gave rise to some challenges regarding sealing, electrode stability, chemical compatibility, start-up and thermal cycling performance, thus limiting the commercialization of SOFCs. To achieve longer life of cell and faster start-up, the operating temperature of the fuel cell must be shifted towards intermediate-to-low temperature (500–800℃). Nevertheless, the oxygen reduction reaction (ORR) and oxygen surface exchange processes are greatly limited by the decline in temperature[3]. A large amount of polarization loss occurs at the cathode. Therefore, the development of high-performance cathode materials for IT-SOFCs is essential.

$LnBaCo_2O_{5+\delta}$ (Ln=Pr, Nd, Sm, Gd, La and Y) oxides with excellent ion-electron mixed conduction, high oxygen surface exchange ($K$) and bulk diffusion ($D$) coefficient have attracted much attention, which can be used promising cathode materials for IT-SOFCs[4-6]. In these perovskite oxides, rare earth ions and alkaline ions took up positions at A site of the lattice[7]. The structure is orderly arranged in sequence of $[BaO][CoO_2][LnO_\delta][CoO_2]$ along $c$-axis. This unique arrangement of ions allows the binding energy of oxygen and rare metal elements to be effectively reduced. But $LnBaCo_2O_{5+\delta}$ perovskite oxides have high coefficients of thermal expansion (CTE) similar to cobalt-based compounds, resulting in the thermal incompatibility with the other SOFC components. The average CTE of $LnBaCo_2O_{5+\delta}$ perovskite oxides are generally $17.6\times10^{-6}$ to $21.5\times10^{-6}$ $K^{-1}$ at 30–800 ℃[5], which is significantly higher than that of electrolytes (*e.g.* $Gd_{0.1}Ce_{0.9}O_{2-\delta}$ (GDC, $13\times10^{-6}$ $K^{-1}$), $(Y_2O_3)_{0.08}(ZrO_2)_{0.92}$ (YSZ, $10.5\times10^{-6}$ $K^{-1}$))[8-9] and cobalt-free cathodes (such as $NdBa_{0.5}Sr_{0.5}Cu_2O_{5+\delta}$, $14.5\times10^{-6}$ $K^{-1}$)[10]. The high CTE of $LnBaCo_2O_{5+\delta}$ mainly comes from two aspects. On the

**Received date:** 2022-09-21; **Revised date:** 2022-11-13; **Published online:** 2022-12-09
**Foundation item:** National Key R&D Program of China (2021YFB4001502); National Natural Science Foundation of China (52272257, 52104229)
**Biography:** GUO Tianmin (1991–), male, Master. E-mail: 277263262@qq.com
郭天民(1991–), 男, 硕士. E-mail: 277263262@qq.com
**Corresponding author:** LING Yihan, professor. E-mail: lyhyy@cumt.edu.cn
凌意瀚, 研究员. E-mail: lyhyy@cumt.edu.cn

one hand, the spin transition of $Co^{3+}$ leads to an increase in the volume of the $CoO_6$ octahedron; on the other hand, plenty of oxygen vacancies are generated during the thermal reduction of Co ions, resulting in lattice expansion[11-12]. Therefore, partially or completely replacing Co with transition metals (Fe, Mn, Cu and Ni) is a feasible approach to depress CTE of $LnBaCo_2O_{5+\delta}$[13-15]. Zhang *et al*.[16] reported that CTE of $GdBaFeNiO_{5+\delta}$ is $14.7\times10^{-6}$ $K^{-1}$ at 30–800 ℃, which is lower than that of $GdBaCo_2O_{5+\delta}$ (GBCO, $20.1\times10^{-6}$ $K^{-1}$) in the same temperature range. But this brings about a decrease in the electrochemical catalytic activity of the oxides.

High-entropy ceramics (HECs) were firstly proposed and joined in high-entropy materials in 2015[17]. HECs are composed of multi-component ceramic compounds[18], and their high structure entropy is beneficial to the formation of HECs. HECs are demonstrated a homogeneous, crystalline, single-phase structure, which makes their properties superior to those of traditional ceramics[19]. Han *et al*.[20] reported that $LaMn_{0.2}Fe_{0.2}Co_{0.2}Ni_{0.2}Cu_{0.2}O_{3-\delta}$(HE-LMO) materials effectively enhanced the electrochemical performance of Sr-free cathode ($LaMnO_{3-\delta}$). Yang *et al*.[21] found that $La_{0.2}Pr_{0.2}Nd_{0.2}Sm_{0.2}Sr_{0.2}MnO_{3-\delta}$ (HE-LSM) suppressed performance degradation caused by Sr segregation. Ling *et al*.[22] researched $SmBa(Mn_{0.2}Fe_{0.2}Co_{0.2}Ni_{0.2}Cu_{0.2})_2O_{5+\delta}$ (HE-SBO) double perovskite oxides, which grievously reduced the CTE of cobalt-based perovskite oxides. Therefore, development of new high-entropy materials to obtain suitable CTE and high-performance cathode for IT-SOFC is feasible. In this work, $GdBa(Fe_{0.2}Mn_{0.2}Co_{0.2}Ni_{0.2}Cu_{0.2})_2O_{5+\delta}$ (HE-GBO) oxide was obtained by uniformly doped with various transition elements at B site to improve ORR reaction activity at intermediate temperature *via* high-entropy effect, its structure and relatively electrochemical properties were explored. Subsequently, GDC was introduced to fabricate HE-GBO-GDC composite cathode for further improving the electrochemical performance of the single cells.

# 1 Experimental

Various metal cation compounds: $Gd_2O_3$, $BaCO_3$, $Co(NO_3)_2{\cdot}6H_2O$, $C_4H_6NiO_4{\cdot}4H_2O$, $(Mn(NO_3)_3)$, $Cu(NO_3)_2{\cdot}3H_2O$, and $Fe(NO_3)_3{\cdot}9H_2O$ were employed to synthesize $GdBa(Co_{0.2}Mn_{0.2}Fe_{0.2}Cu_{0.2}Ni_{0.2})_2O_{5+\delta}$ (HE-GBO) by the self-propagating combustion method, and the specific preparation process has been introduced in our previous work[23]. Then, to obtain the pure phase of this powder, the primary powder was sintered at 1150 ℃ for 3 h.

The dendritic anode was prepared using phase inversion technology[24]. Commercial NiO and YSZ were blended with 0.216 g of poly-vinylpyrrolidone and 14.16 g solution of 1-methyl-2-pyrrolidinone (NMP) and polyether sulfone (PESF) (mass ratio 17.7:100) to acquire a homogenous slurry. Two parts of the slurries were placed in a mold and separated by a stainless-steel mesh ($\phi$150 μm), and water was poured into the mold at a constant speed. After being left for 2.5–3.0 h, the raw substrate was taken out of the mold, soaked in water for 12 h and dried at 50 ℃. The dried raw substrate was sintered at 1050 ℃ for 2 h. Then YSZ electrolyte slurry was spin-coated 3 times on the anode substrate, and sintered at 1400 ℃ for 10 h. The YSZ slurry was fabricated with 10 g YSZ, 0.2 g polyester/polyamine copolymer (KD-1) and some acetone as solvent with ball milling for 10 h. After the addition of 20 g terpineol ethyl cellulose (5%), the sample was further milled for 12 h. The preparation method of GDC slurry is the same as the above-mentioned YSZ slurry, coated on the YSZ and sintered at 1250 ℃ for 3 h. Subsequently, cathode slurry was coated on GDC, and sintered at 950 ℃ for 3 h. The active area of cathode was 0.24 $cm^2$. HE-GBO slurry was manufactured by hand milling 1 g HE-GBO powder with 1.5 g terpineol ethyl cellulose (10%). The synthesized HE-GBO powder was mixed with 30% (in mass) GDC to acquire composite cathode slurry.

X-ray diffractometer (XRD, Bruker 8 ADVANCE, Germany) was used to analyze the characteristic of GBCO, HE-GBO and the relatively chemical compatibility with YSZ and GDC, respectively. GBCO and HE-GBO powders were compressed to form cuboid bars in mold, respectively, and calcined at 1150 ℃ for 5 h for CTE measurement by a thermal dilatometer (DIL402PC, Germany). The electrochemical data of cells were collected using an electrochemical workstation (ZAHNER, Germany). The structures of fuel cells were observed by a scanning electron microscope (SEM, Gemini-300, Germany). The energy dispersive spectroscopy (EDS) mapping was explored by X-ray spectroscope (Oxford Instruments AZtecEnergy, England).

# 2 Results and discussion

XRD patterns of HE-GBO and GBCO oxides are shown in Fig. 1. The result indicate that HE-GBO is a single-phase double perovskite without any impurities after calcined at 1150 ℃ for 3 h. Previous studies demonstrated that GBCO belongs to an orthogonal structure[25-26]. The difference in the XRD patterns of GBCO and HE-GBO comes from the change in crystal structures, which suggests that the crystal structure of HE-GBO transform into a tetragonal structure(P4/mmm)[16]. Schematic diagram of the HE-GBO double perovskite structure is shown in Fig. 1(c).

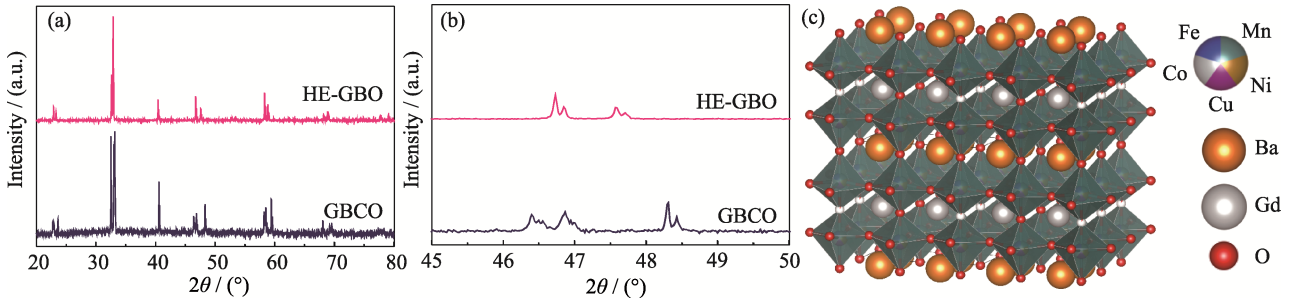


Fig. 1 (a) XRD patterns and (b) corresponding magnified area of $2\theta$=45°–50° of GBCO and HE-GBO powders calcined at 1150 ℃ for 3 h, and (c) schematic diagram of the HE-GBO double perovskite structure

Chemical compatibility of HE-GBO and YSZ was explored by sintering HE-GBO-YSZ mixtures (mass ratio 1∶1) powder at 950 ℃ for 3 h, as shown in Fig. 2(a). There are some new reaction phases except HE-GBO and YSZ, indicating that HE-GBO is chemically incompatible with YSZ at 950 ℃. In Fig. 2(b), all diffraction peaks of HE-GBO-GDC mixtures (mass ratio 1∶1) come from the peaks of HE-GBO and GDC, and no new diffraction peak and position shifts are observed, suggesting that HE-GBO is chemically compatible with GDC. Therefore, GDC can be a good barrier layer between YSZ and HE-GBO to prevent side reactions.

Thermal expansion curves of GBCO and HE-GBO from 25 ℃ to 800 ℃ measured under the same condition are shown in Fig. 3. CTE of HE-GBO is $15.7\times10^{-6}$ $K^{-1}$, which presents relatively reduced CTE compared with

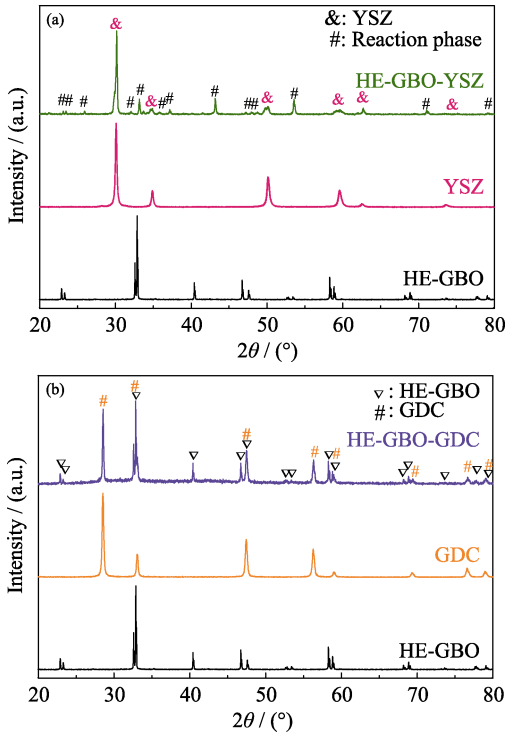


Fig. 2 XRD patterns of chemical compatibility between cathode (HE-GBO) and electrolytes materials (YSZ and GDC) calcined at 950 ℃ in air

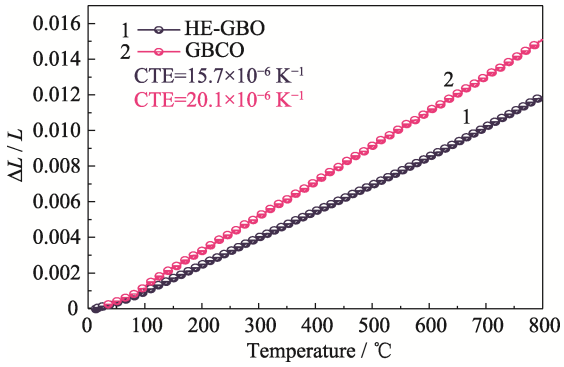


Fig. 3 Temperature dependence of average CTE of GBCO and HE-GBO in air from 25 to 800 ℃
Colorful figure is available on website

GBCO ($20.1\times10^{-6}$ $K^{-1}$). In HE-GBO, Co is partially replaced by other transition metal elements (Fe, Mn, Ni and Cu), which weakens the influence of the spin state transition of Co ions. Meanwhile, the serious lattice distortion impedes the oscillation amplitude of constituent atoms, resulting in a significant decrease in the CTE of HE-GBO[27]. Preparation of HE-GBO-GDC composites by addition of GDC can further meet the requirements of thermal expansion matching with electrolytes. Related reports have demonstrated the feasibility of GDC composite electrode materials[28].

Electrochemical impedance spectroscopy (EIS) plots of symmetrical cells using HE-GBO and HE-GBO-GDC as cathodes in air are shown in Fig. 4. The intersection point of the high-frequency and low-frequency impedance arc with $x$-axis represents Ohmic impedance ($R_\Omega$) and total impedance ($R_t$), respectively. Polarization impedance ($R_p$) can be obtained by subtracting $R_\Omega$ from $R_t$. $R_\Omega$ is not discussed and set to zero. $R_p$ of HE-GBO are 1.68, 2.80, 8.28, 27.20 and 98.53 Ω·$cm^2$, and $R_p$ of HE-GBO-GDC electrode are 0.23, 0.53, 0.82, 4.00 and 12.58 Ω·$cm^2$ at 800–600 ℃, respectively, indicating that HE-GBO-GDC composite cathode possesses higher electrochemical performance than HE-GBO. Because the introduction of the oxygen-ion conductive phase (GDC) in HE-GBO can increase the three-phase interface (TPB) for the oxygen reduction reaction[29].

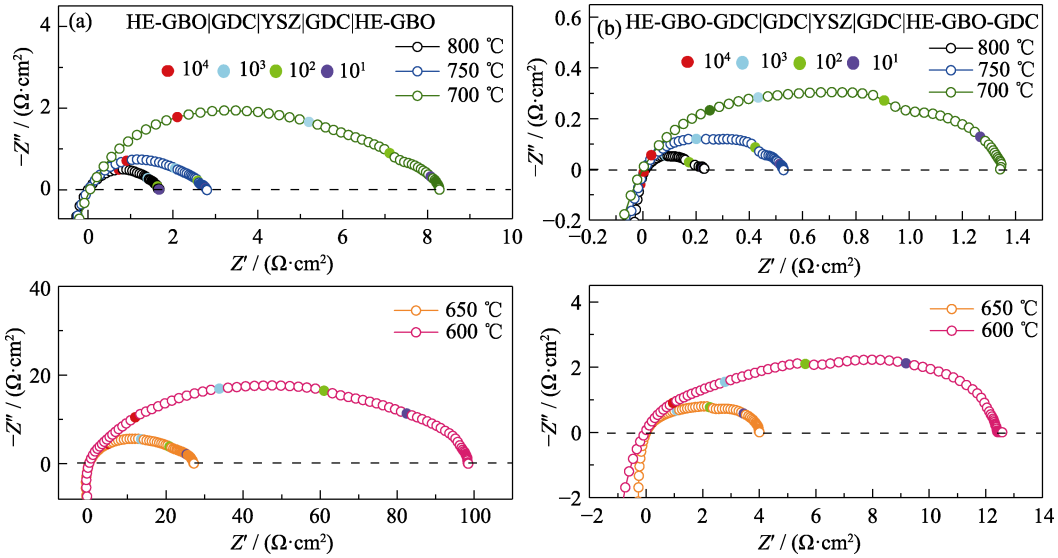


Fig. 4 EIS plots of symmetrical single cells with (a) HE-GBO and (b) HE-GBO-GDC cathodes measured from 800 to 600 ℃ in air
Colorful figures are available on website

The gas mass transfer can be greatly improved using vertical microscopic channels Ni-YSZ anodes[30]. The microstructures of the cell with HE-GBO and HE-GBO-GDC cathodes after 100 h of long-term testing exhibit in Fig. 5(a, b), respectively. Both single cells consist of 4 components (Ni-YSZ, YSZ, GDC and LSCF-GDC), and components are in good contact.

YSZ electrolyte achieves densification to distinguish the anode and cathode gas atmospheres, and its thickness is about 14 μm. The thickness of the GDC barrier is around 8 μm. Both cells have similar microstructures. SEM microstructures of HE-GBO and HE-GBO-GDC cathodes are given in Fig. 5(c, d) to perform the stability after testing, respectively. HE-GBO displays a loose and porous structure, and the porosity of HE-GBO composite cathode decreases with the addition of GDC. GDC particles uniformly cover the surface of HE-GBO, enlarging the effective area of three-phase interface and reducing $R_p$ of the single cell. The associated EDS spectra of HE-GBO cathode after long-term testing can be observed in Fig. 6. Gd, Ba, Co, Fe, Ni, Mn, and Cu elements are distributed homogeneously.

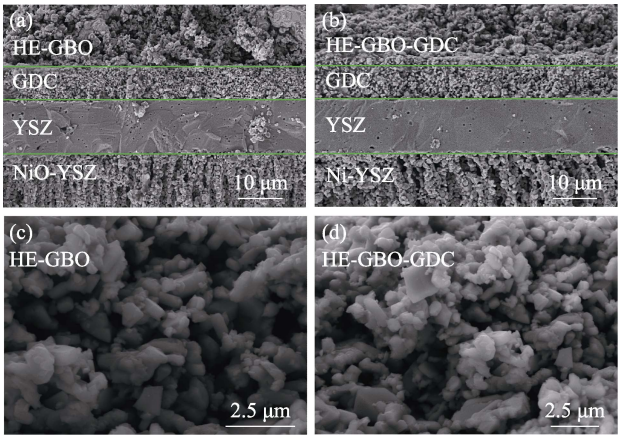


Fig. 5 Cross-section morphologies of single cell with (a) HE-GBO and (b) HE-GBO-GDC after 100 h long-term test, and (c, d) their magnified morphologies, respectively

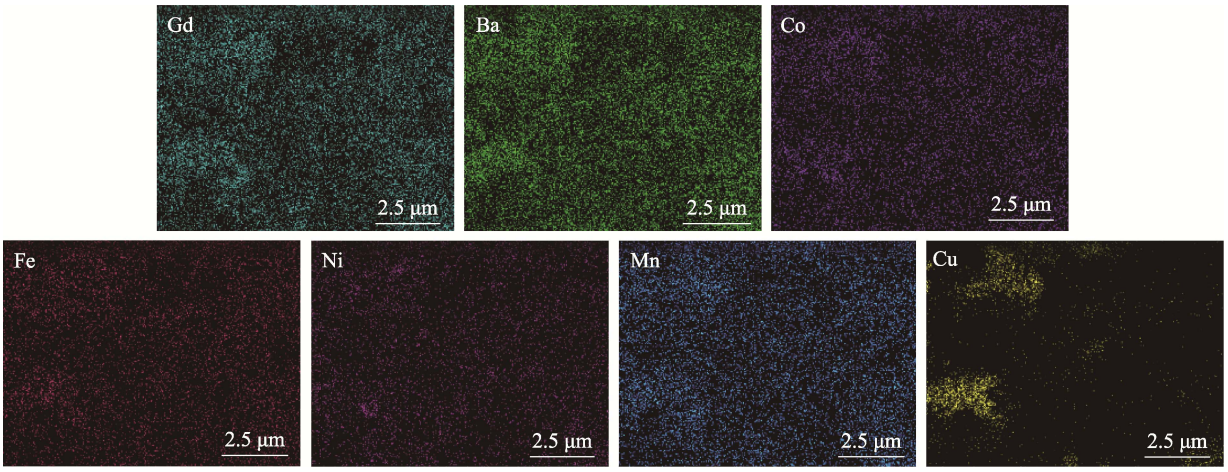


Fig. 6 EDS surface sweep results for high-entropy cathode material (HE-GBO, in Fig. 5(c)) after 100 h long-term test

The electrochemical performance of the cell with HE-GBO and HE-GBO-GDC cathodes is characterized by using wet hydrogen (~3% $H_2O$) as fuel at 800–600 ℃ in Fig. 7(a, b), respectively. The open circuit voltages (OCVs) of the cells with HE-GBO and HE-GBO-GDC in wet $H_2$ atmosphere are 1.086 and 1.071 V at 800 ℃, respectively. The maximum power densities ($P_{max}$) of single cell with HE-GBO as cathode are 972.12, 638.76, 417.39, 211.53, and 105.23 mW/cm$^2$ at 800–600 ℃, respectively. $P_{max}$ of single cell with HE-GBO-GDC composite cathode are 1057.06, 745.19, 456.09, 249.66 and 122.28 mW/cm$^2$ at 800–600 ℃. $P_{max}$ of single cell with HE-GBO-GDC composite cathode is 8% higher than that of single cell with HE-GBO single-phase cathode at 800 ℃, attributed to lower $R_p$ and CTE of HE-GBO-GDC composite cathode compared to HE-GBO. Lower CTE of the composite cathode is beneficial to improving the bonding performance with the electrolyte and enhancing the oxygen ion migration ability, thereby increasing the electrochemical performance. Due to its high performance and fine thermal expansion compatibility with the electrolyte, HE-GBO-GDC is a further promising cathode for IT-SOFC.

The relevant EIS plots of single cell with HE-GBO and HE-GBO-GDC cathodes measured at OCV exhibit in Fig. 8(a, b), respectively. $R_\Omega$ and $R_p$ increase with the

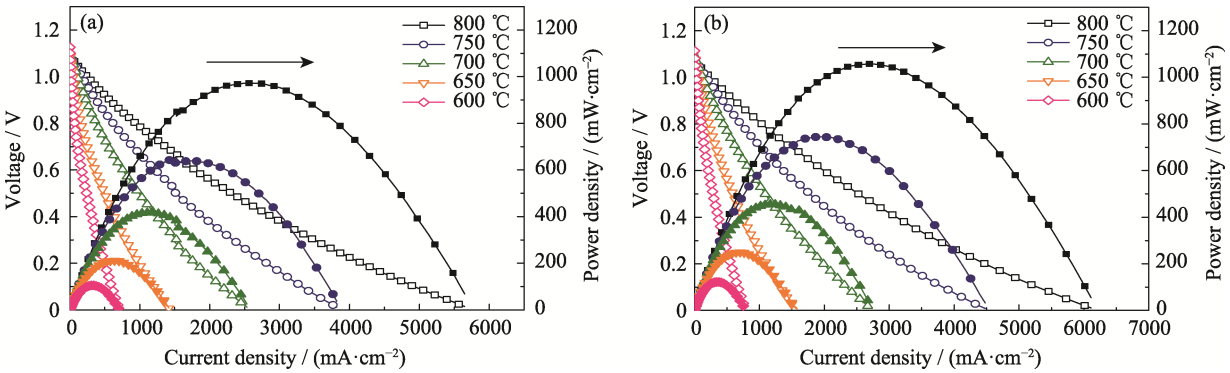


Fig. 7 *I-V* and *I-P* curves of single cells with (a) HE-GBO and (b) HE-GBO-GDC cathodes measured from 800 ℃ to 600 ℃ in wet $H_2$ (~3% $H_2O$)

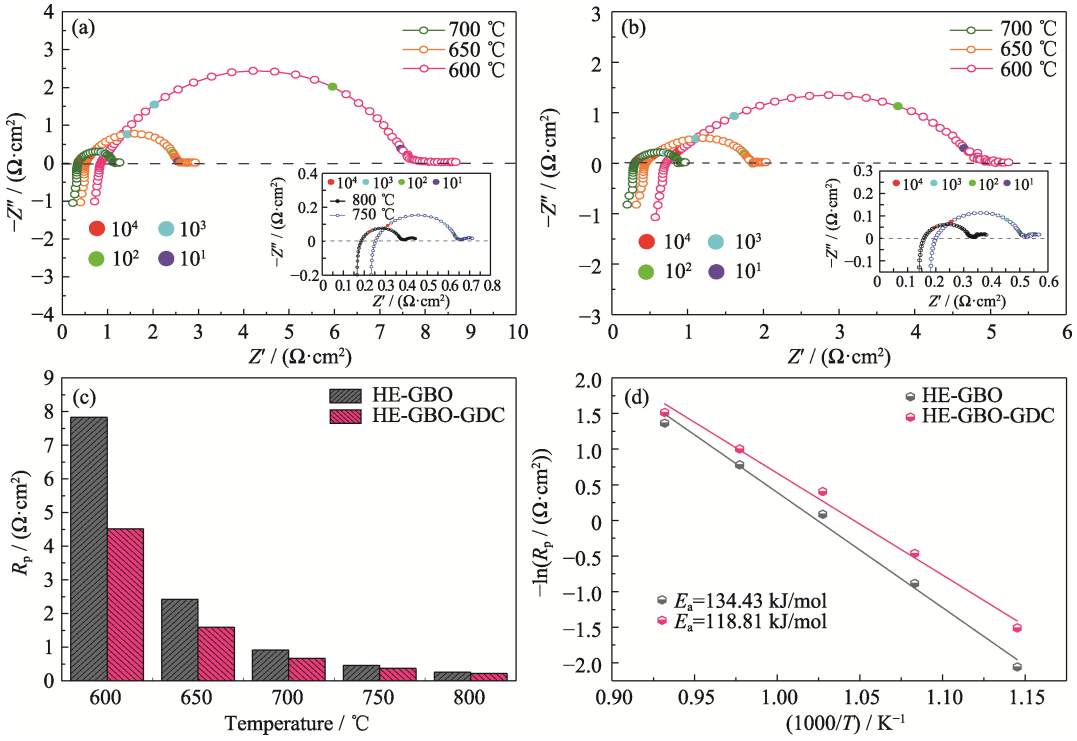


Fig. 8 EIS plots of single cells with (a) HE-GBO and (b) HE-GBO-GDC cathodes measured from 800 ℃ to 600 ℃ in wet $H_2$ (~3% $H_2O$), (c) simulated polarization resistance, and (d) Arrhenius plots of single cells with HE-GBO and HE-GBO-GDC cathodes

Colorful figures are available on website

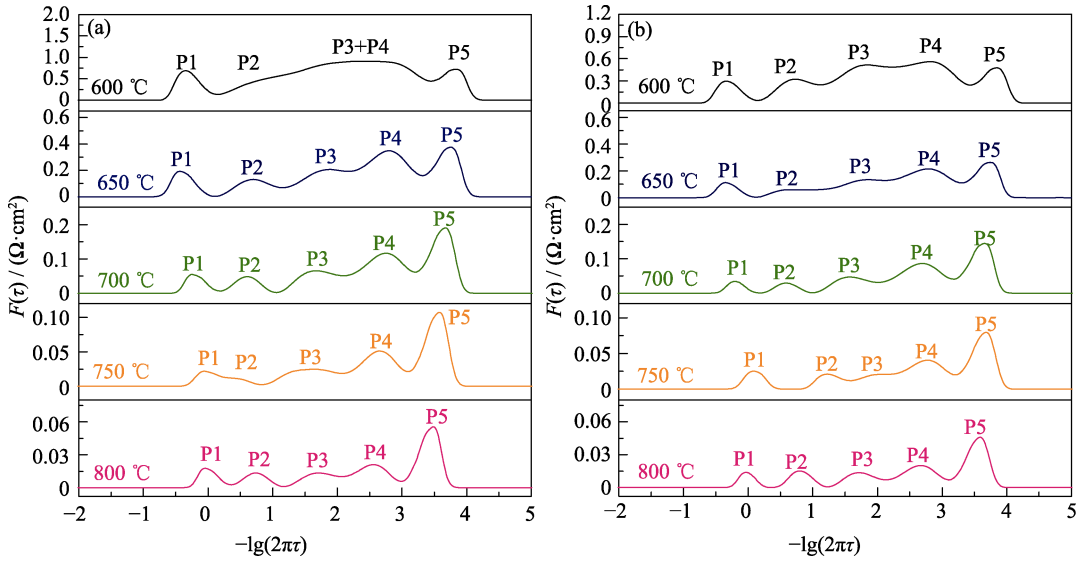


Fig. 9 DRT analysis of EIS data for the single cells with (a) HE-GBO and (b) HE-GBO-GDC cathodes from 800–600 ℃

decrease of temperature. It is known that $R_p$ of the anode-supported single cells which mainly derived from the polarization process of the cathode can directly reflect the cathode ORR activity[31]. $R_p$ of single cells with HE-GBO cathode increases from 0.26 to 7.83 Ω·cm$^2$ at 800–600 ℃. For HE-GBO-GDC cathode, $R_p$ increases from 0.22 to 4.52 Ω·cm$^2$ at 800–600 ℃ (Fig. 8(c)). HE-GBO-GDC composite cathode can enhance the electrochemical performance of the cell, which is due to the effect of GDC as mixed conductor of ions and electrons. It improves the diffusion rate of oxygen ions and increase the three-phase interface of ORR. The results of activation energy ($E_a$) for $R_p$ by Arrhenius equation are shown in Fig. 8(d), $E_a$ of HE-GBO and HE-GBO-GDC cathode are 134.43 and 118.81 kJ/mol, respectively.

To further evaluate the difference in $R_p$ of the cell with HE-GBO and HE-GBO-GDC cathodes, distribution of relaxation time (DRT) is employed to analyze EIS in Fig. 9(a, b). DRT curves are divided into five peaks in the measured frequency field and defined as P1, P2, P3, P4 and P5. Among them, P1 may be related to hydrogen and oxygen diffusion within electrodes at low frequency[32]. P2 peak is taken as the gas adsorption in the electrode. P3 and P4 peaks are associated with gas adsorption as well as oxygen reduction and diffusion of oxygen ions into electrolyte[33-34]. P5 is ascribed to gas adsorption and diffusion of oxygen ions to TPB. As shown in Fig. 9(b), $R_p$ of single cell with HE-GBO-GDC decreases at each rate-limiting step, suggesting that the addition of GDC is beneficial, and the improvement in catalytic performance of the HE-GBO-GDC becomes more pronounced with decreasing temperature. Weakening of P4 and P5 peaks may be attributed to the addition of the ionic conductive phase GDC.

The long-term testing of the single cell with HE-GBO cathode in $H_2$ (~3% $H_2O$) atmosphere was detected (Fig. 10). The voltages of the single cell under 200 mA/cm$^2$ show no attenuation after 100 h long-term measurement, which indicates that the high-entropy oxide as cathode has good stability on the foundation of high performance and owns a proper prospect for the application of IT-SOFCs.

## 4 Conclusion

This work proposes a high-entropy double perovskite cathode of $GdBa(Fe_{0.2}Mn_{0.2}Co_{0.2}Ni_{0.2}Cu_{0.2})_2O_{5+\delta}$ (HE-GBO) to solve the conflict problem of thermal compatibility and catalytic activity in IT-SOFCs.

1) HE-GBO material is successfully synthesized *via* self-propagating combustion method and matches with GDC at operating temperatures. GDC is introduced into HE-GBO to prepare composite cathode.

2) Through doping multiple transition metal cations at B-site, HE-GBO material presents superior CTE ($15.7\times10^{-6}$ K$^{-1}$) compared with $GdBaCo_2O_{5+\delta}$, suggesting that the high

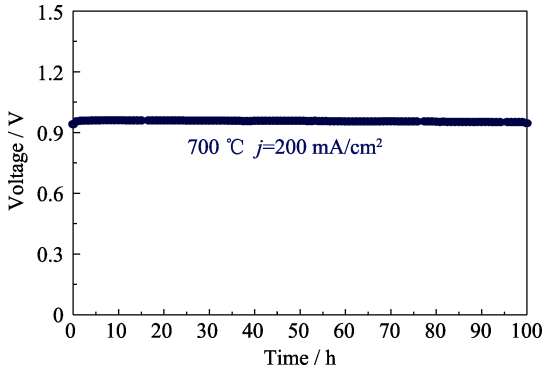


Fig. 10 Long-term stability performance of single cell with HE-GBO cathode in $H_2$ (~3% $H_2O$) atmosphere

entropy effect can significantly reduce CTE, and matches state-of-the-art electrolytes.

3) $P_{max}$ of the single cells with HE-GBO-GDC is 8% higher than that of HE-GBO at 800 ℃, indicating the high-entropy cathodes are promising for compatibility-activity balance in IT-SOFC.

## References:


[1] STEELE B C H, HEINZEL A. Materials for fuel-cell technologies. *Nature*, 2001, **414(6861):** 345.

[2] GUO M, TU H, LI S, YU Q, *et al.* Fabrication and characterization of functionally graded cathodes based on *in-situ* formed $La_{0.6}Sr_{0.4}CoO_{3-\delta}$ for intermediate temperature SOFCs. *Journal of Inorganic Materials*, 2014, **29(6):** 621.

[3] LING Y, GUO T, GUO Y, *et al.* New two-layer Ruddlesden-Popper cathode materials for protonic ceramics fuel cells. *Journal of Advanced Ceramics*, 2021, **10(5):** 1052.

[4] LIU F, ZHAO Z, MA Y, *et al.* Robust Joule-heating ceramic reactors for catalytic CO oxidation. *Journal of Advanced Ceramics*, 2022, **11(7):** 1163.

[5] ZHOU Q, WANG F, SHEN Y, *et al.* Performances of $LnBaCo_2O_{5+\delta}$-$Ce_{0.8}Sm_{0.2}O_{1.9}$ composite cathodes for intermediate temperature solid oxide fuel cells. *Journal of Power Sources*, 2010, **195(8):** 2174.

[6] JIN H, WANG H, ZHANG H, *et al.* Synthesis and characterization of $GdBaCo_2O_{5+\delta}$ cathode material by glycine-nitrate process. *Journal of Inorganic Materials*, 2012, **27(7):** 751.

[7] TAN Y, WANG R, HU X, *et al.* Comparison of the oxygen reduction mechanisms in a GBCO-SDC-impregnated cathode and a GBCO cathode. *Journal of Applied Electrochemistry*, 2019, **49(10):** 1035.

[8] ZHOU Q, ZHANG Y, SHEN Y, *et al.* Layered perovskite $GdBaCuCoO_{5+\delta}$ cathode material for intermediate-temperature solid oxide fuel cells. *Journal of the Electrochemical Society*, 2010, **157(5):** B628.

[9] DING X, CUI C, GUO L. Thermal expansion and electrochemical performance of $La_{0.7}Sr_{0.3}CuO_{3-\delta}$-$Sm_{0.2}Ce_{0.8}O_{2-\delta}$ composite cathode for IT-SOFCs. *Journal of Alloys and Compounds*, 2009, **481(1/2):** 845.

[10] KONG X, LIU G, YI Z, *et al.* $NdBaCu_2O_{5+\delta}$ and $NdBa_{0.5}Sr_{0.5}Cu_2O_{5+\delta}$ layered perovskite oxides as cathode materials for IT-SOFCs. *International Journal of Hydrogen Energy*, 2015, **40(46):** 16477.

[11] BURLEY J, MITCHELL J, SHORT S, *et al.* Structural and magnetic chemistry of $NdBaCo_2O_{5+\delta}$. *Journal of Solid State Chemistry*, 2003, **170(2):** 339.

[12] ASAI K, YONEDA A, YOKOKURA O, *et al.* Two spin-state transitions in $LaCoO_3$. *Journal of the Physical Society of Japan*, 1998, **67(1):** 290.

[13] KIM Y, MANTHIRAM A. Layered $LnBaCo_{2-x}Cu_xO_{5+\delta}$ ($0 \leqslant x \leqslant 1.0$) perovskite cathodes for intermediate-temperature solid oxide fuel cells. *Journal of the Electrochemical Society*, 2010, **158(3):** B276.

[14] HUANG X, FENG J, ABDELLATIF H R, *et al.* Electrochemical evaluation of double perovskite $PrBaCo_{2-x}Mn_xO_{5+\delta}$ ($x$=0, 0.5, 1) as promising cathodes for IT-SOFCs. *International Journal of Hydrogen Energy*, 2018, **43(18):** 8962.

[15] JIN F, LI J, WANG Y, *et al.* Evaluation of Fe and Mn co-doped layered perovskite $PrBaCo_{2/3}Fe_{2/3}Mn_{1/2}O_{5+\delta}$ as a novel cathode for intermediate-temperature solid-oxide fuel cell. *Ceramics International*, 2018, **44(18):** 22489.

[16] LI L, JIN F, SHEN Y, *et al.* Cobalt-free double perovskite cathode $GdBaFeNiO_{5+\delta}$ and electrochemical performance improvement by $Ce_{0.8}Sm_{0.2}O_{1.9}$ impregnation for intermediate-temperature solid oxide fuel cells. *Electrochimica Acta*, 2015, **182:** 682.

[17] ROST C M, SACHET E, BORMAN T, *et al.* Entropy-stabilized oxides. *Nature Communications*, 2015, **6(1):** 8485.

[18] YANG Y, MA L, GAN G Y, *et al.* Investigation of thermodynamic properties of high entropy (TaNbHfTiZr)C and (TaNbHfTiZr)N. *Journal of Alloys and Compounds*, 2019, **788:** 1076.

[19] OSES C, TOHER C, CURTAROLO S. High-entropy ceramics. *Nature Reviews Materials*, 2020, **5(4):** 295.

[20] HAN X, YANG Y, FAN Y, *et al.* New approach to enhance Sr-free cathode performance by high-entropy multi-component transition metal coupling. *Ceramics International*, 2021, **47(12):** 17383.

[21] YANG Y, BAO H, NI H, *et al.* A novel facile strategy to suppress Sr segregation for high-entropy stabilized $La_{0.8}Sr_{0.2}MnO_{3-\delta}$ cathode. *Journal of Power Sources*, 2021, **482:** 228959.

[22] LING Y, HAN X, YANG Y, *et al.* Stable high-entropy double perovskite cathode $SmBa(Mn_{0.2}Fe_{0.2}Co_{0.2}Ni_{0.2}Cu_{0.2})_2O_{5+\delta}$ for intermediate-temperature solid oxide fuel cells. *Journal of the Chinese Ceramic Society*, 2022, **50(1):** 219.

[23] SONG W, MA Z, YANG Y, *et al.* Characterization and polarization DRT analysis of direct ethanol solid oxide fuel cells using low fuel partial pressures. *International Journal of Hydrogen Energy*, 2020, **45(28):** 14480.

[24] SHAO X, RICKARD W D, DONG D, *et al.* High performance anode with dendritic porous structure for low temperature solid oxide fuel cells. *International Journal of Hydrogen Energy*, 2018, **43(37):** 17849.

[25] ZHANG K, GE L, RAN R, *et al.* Synthesis, characterization and evaluation of cation-ordered $LnBaCo_2O_{5+\delta}$ as materials of oxygen permeation membranes and cathodes of SOFCs. *Acta Materialia*, 2008, **56(17):** 4876.

[26] KIM J H, MANTHIRAM A. Layered $NdBaCo_{2-x}Ni_xO_{5+\delta}$ perovskite oxides as cathodes for intermediate temperature solid oxide fuel cells. *Electrochimica Acta*, 2009, **54(28):** 7551.

[27] ZHAO Z, CHEN H, XIANG H, *et al.* High entropy defective fluorite structured rare-earth niobates and tantalates for thermal barrier applications. *Journal of Advanced Ceramics*, 2020, **9(3):** 303.

[28] LEE S J, KIM D S, JO S H, *et al.* Electrochemical properties of $GdBaCo_{2/3}Fe_{2/3}Cu_{2/3}O_{5+\delta}$-CGO composite cathodes for solid oxide fuel cell. *Ceramics International*, 2012, **38:** S493.

[29] LI S, ZHANG L, XIA T, *et al.* Synergistic effect study of $EuBa_{0.98}Co_2O_{5+\delta}$-$Ce_{0.8}Sm_{0.2}O_{1.9}$ composite cathodes for intermediate-temperature solid oxide fuel cells. *Journal of Alloys and Compounds*, 2019, **771:** 513.

[30] YANG Y, LIU Y, CHEN Z, *et al.* Enhanced conversion efficiency and coking resistance of solid oxide fuel cells with vertical-microchannel anode fueled in $CO_2$ assisted low-concentration coal-bed methane. *Separation and Purification Technology*, 2022, **288:** 120665.

[31] DAI T, SUN B, YI Q, *et.al*. The effect of pore former on the microstructure and performance of SOFC cathode. *Guangzhou Chemical Industry*, 2013, **41:**7.

[32] LI T, YANG Y, WANG X, *et al.* Enhance coking tolerance of high-performance direct carbon dioxide-methane solid oxide fuel cells with an additional internal reforming catalyst. *Journal of Power Sources*, 2021, **512:** 230533.

[33] KORNELY M, MENZLER N, WEBER A, *et al.* Degradation of a high performance SOFC cathode by Cr-poisoning at OCV-conditions. *Fuel Cells*, 2013, **13(4):** 506.

[34] LIU B, MUROYAMA H, MATSUI T, *et al.* Analysis of impedance spectra for segmented-in-series tubular solid oxide fuel cells. *Journal of the Electrochemical Society*, 2010, **157(12):** B1858.

# 中温固体氧化物燃料电池的高熵双钙钛矿阴极材料: 兼容性与活性研究

郭天民[1], 董江波[2], 陈正鹏[2], 饶睦敏[2], 李明飞[2], 李 田[1], 凌意瀚[1]

(1. 中国矿业大学 材料科学与物理学院, 徐州 221116; 2. 广东能源集团科技研究院有限公司, 广州 510000)

**摘 要:** 中温固体氧化物燃料电池(IT-SOFC)有助于国家的碳中和战略, 但其阴极材料难以兼顾热兼容性和催化活性。为此, 基于多元素耦合的高熵策略, 本研究合成了高熵阴极材料 $GdBa(Fe_{0.2}Mn_{0.2}Co_{0.2}Ni_{0.2}Cu_{0.2})_2O_{5+\delta}$(HE-GBO), 具有双过氧化物结构, 与 $Gd_{0.1}Ce_{0.9}O_{2-\delta}$(GDC)有良好的化学兼容性, 协调了与催化活性之间的平衡性。采用 HE-GBO 阴极的对称电池在 800 ℃下的极化电阻($R_p$)为 1.68 Ω·cm$^2$, 而 HE-GBO-GDC(质量比 7∶3)复合阴极的 $R_p$ 因引入 GDC 而显著降低(800 ℃下 $R_p$ 为 0.23 Ω·cm$^2$)。采用 HE-GBO 和 HE-GBO-GDC 阴极组装树枝状微通道阳极支撑单电池,在 800 ℃的最大功率密度分别达到 972.12 和 1057.06 mW/cm$^2$, 使用高熵阴极可以进一步提高电池性能。这些结果表明多尺度优化有助于开发高性能的 IT-SOFC 阴极材料。

**关 键 词:** 高熵阴极; 固体氧化物燃料电池; 热相容性; 树枝状微通道

**中图分类号:** O61 **文献标志码:** A